

Multi-wavelength emission from Jets and Magnetically Arrested Disks in Radio Galaxies

Riku Kuze,^{1,*} Shigeo S. Kimura^{1,2} and Kenji Toma^{1,2}

¹*Astronomical Institute, Graduate School of Science, Tohoku University, Sendai 980-8578, Japan*

²*Frontier Research Institute for Interdisciplinary Sciences, Tohoku University, Sendai 980-8578, Japan*

E-mail: r.kuze@astr.tohoku.ac.jp, shigeo@astr.tohoku.ac.jp,
toma@astr.tohoku.ac.jp

The emission mechanisms and regions of multi-wavelength photons from radio galaxies are unknown. The emission from Magnetically Arrested Disks (MADs) with strong magnetic fields at the center of radio galaxies can explain the high-energy gamma-ray data, but the MAD model cannot explain the observational X-ray data. One possible scenario to explain radio to X-ray data is the emission from jets. We construct the Jet-MAD model taking into account the multi-wavelength emission from the jets and from the MADs with the particle injection model based on magnetic reconnection in the black hole magnetosphere. We apply the Jet-MAD model to M87 and compare it with the simultaneous multi-wavelength observational data. We consider the two-acceleration mechanism inside the jet: magnetic reconnection and Alfvén wave dissipation. We find that the Jet-MAD model can explain the radio to gamma-ray observational data with the magnetic reconnection scenario, but the Jet-MAD model cannot explain the observational data with the Alfvén wave dissipation scenario. We conclude that the magnetic reconnection likely accelerates the particles inside the jet.

38th International Cosmic Ray Conference (ICRC2023)
26 July - 3 August, 2023
Nagoya, Japan



*Speaker

1. Introduction

Radio-loud active galactic nuclei (AGNs) have powerful relativistic jets. These AGNs emit from radio to GeV–TeV gamma rays, but the emission mechanism and region are still unknown. The emission mechanism in radio galaxies is considered the synchrotron radiation and the inverse Compton scattering by particles accelerated by the internal shock in the jets as the standard scenario. However, if we try to explain the observational data by the leptonic jet model, the required magnetic field to explain the observational data is lower than that estimated by the observation of the radio core shift ([1]). Another scenario is proposed that the hadronic emission from the Magnetically Arrested Disks (MADs) around the central supermassive black hole (BH) ([2]). The MAD model can explain the gamma-ray observational data, but cannot explain the radio and X-ray data ([3]). We consider the radio to X-rays to come from the jets, and thus, we construct the model of multi-wavelength emission from jets and accretion disks by using the particle injection model ([4], [5]). In the injection model, the particles are accelerated by the magnetic reconnection nearby the BH magnetosphere ([6]). The accelerated particles emit photons that produce electron-positron pairs via two-photon interaction($\gamma + \gamma \rightarrow e^+ + e^-$), and thus the injection model considers that the produced electron-positron pairs are injected into the jet.

We explain the Jet-MAD model in section 2. In section 3, we apply this model to M87 and change the acceleration mechanism to investigate which mechanism is likely by comparing the photon spectra obtained by the Jet-MAD model and the simultaneous multi-wavelength observational data. Section 4 we summarize and discuss the Jet-MAD model.

2. Jet-MAD Hybrid Model

We show the schematic image of the Jet-MAD model in Fig.1. In the MADs, particles are accelerated by the magnetic reconnection in the accretion flows and emit broadband photons via synchrotron radiation. The magnetic reconnection also occurs in the vicinity of the BH and accelerates the particles that emit the photons. The electron-positron pairs produced by the two-photon interaction form the blob. The blob propagates along the magnetic field lines. The acceleration mechanism in the blob is unknown. The velocity difference between the blob and the ambient gas causes Kelvin-Helmholtz instability (KHI), and we consider that magnetic reconnection occurs due to turbulence. We consider that magnetic reconnection accelerates the particles, and they emit the photons from radio to X-rays via synchrotron radiation.

2.1 MAD model

In this section, we explain the radiation mechanism of the MAD model (see also [2] and [3]). In the MAD, we consider the high-temperature plasma accretes onto the BH of mass M_{BH} . The mass accretion rate \dot{m} and the radiation region R are normalized by the Eddington rate and the gravitational radius, respectively, i.e., $\dot{M}c^2 = \dot{m}L_{\text{Edd}}$, $R = rR_g = rGM/c^2$. We use the notation $Q_x = Q/10^x$ except for the BH mass, M ($M_9 = M_{\text{BH}}/(10^9 M_{\odot})$). We consider electrons and protons to be accelerated by the magnetic reconnection at the edge of the accretion flow and emit multi-wavelength photons via synchrotron radiation. We determine the temperature of the thermal electrons by using the balance between the heating rate and the radiative cooling

rate. Thermal electrons emit radio to UV via synchrotron radiation and Comptonization. We consider the differential number density of nonthermal particles to be power-law whose power-law index is s_{inj} . Nonthermal electrons and protons emit the X-rays to MeV gamma-rays and GeV gamma-rays, respectively. Nonthermal protons interact with the radio via the Bethe-Heitler process ($p + \gamma \rightarrow p + e^+ + e^-$) and produce electron-positron pairs. The electron-positron pairs produced by the Bethe-Heitler process emit TeV-gamma rays via synchrotron radiation. TeV gamma-rays interact with optical by the two-photon interactions ($\gamma + \gamma \rightarrow e^+ + e^-$). The electron-positron pairs produced by the two-photon interaction emit X-rays to MeV gamma-rays via synchrotron radiation.

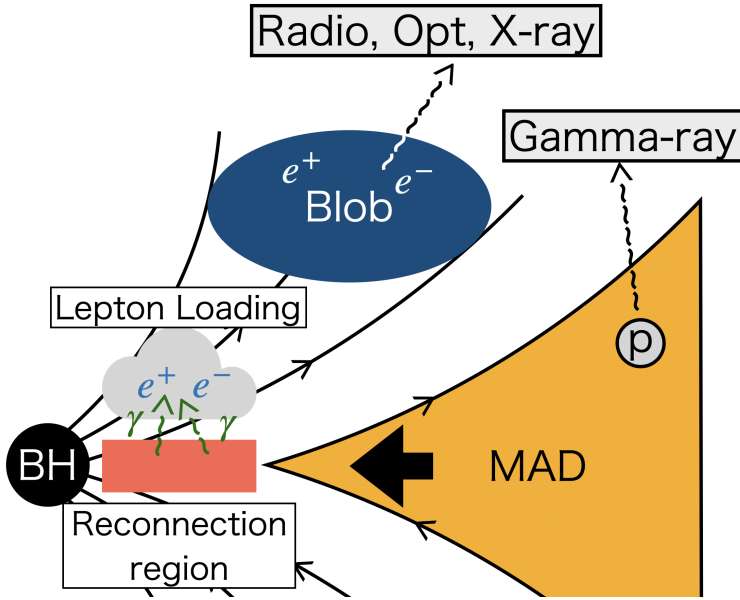


Figure 1: Schematic image of the Jet-MAD model. Magnetic reconnection in the vicinity of the BH accelerates the particles, and the particles emit the photons via synchrotron radiation. Radio blob consists of electron-positron pairs produced by the two-photon interaction. Electrons inside the blob emit radio, opt, and X-rays via synchrotron radiation. Protons in the MADs emit gamma rays via synchrotron radiation.

2.2 Dynamical properties

We consider that magnetic field strength around the BH that has the MAD is estimated to be $B_{\text{mad}} = \sqrt{\dot{M}c\Phi_{\text{mad}}^2/(4\pi^2 r_g^2)} \simeq 1.1 \times 10^3 M_9^{-1/2} \dot{m}_{-4}^{1/4} \Phi_{\text{mad},1.7}$ G, where $\Phi_{\text{mad}} \simeq 50\Phi_{\text{mad},1.7}$ is the saturated magnetic flux of the MAD. High-resolution general relativistic magnetohydrodynamics simulations with a BH spin parameter $a = 0.935$ suggests that the magnetic reconnection occurs in a radius $r_{\text{rec}} \approx 2R_g$, and we fix the $r_{\text{rec}} = 2R_g$ in this study for simplicity. We estimate the reconnecting magnetic field to be $B_{\text{rec}} = \sqrt{2}B_{\text{mad}}(r_{\text{rec}}/r_g)^{-2} \simeq 3.9 \times 10^3 M_9^{-1/2} \dot{m}_{-4}^{1/2} \Phi_{\text{rec},1.2}$ G, where $\Phi_{\text{rec}} = \sqrt{2}\Phi_{\text{mad}}(r_{\text{rec}}/r_g)^{-2}$ is the magnetic flux in the magnetic reconnection region. In [5], the maximum energy of the particles is assumed as $\gamma_{\text{max}} = 4\sigma$ due to the dissipation of the magnetic energy via magnetic reconnection. In this study, we estimate the steady-state σ by solving the Eq.(20) of [5], where $B = B_{\text{rec}}$, $\ell = \ell_{\text{rec}} \approx r_g$. This σ is the value at the base of the jet. We assume the magnetization parameter at the dissipation region as the free parameter $\tilde{\sigma}$. At the

dissipation region, proton and electrons are injected into the blob from the ambient gas due to the KHI, and thus, $\tilde{\sigma}$ can be less than 1.

We assume the radius of the blob in the dissipation region to be R_b . The equation of energy conservation is written as

$$L_j = (\epsilon_e + \epsilon_p + \epsilon_B) \pi R_b^2 c, \quad (1)$$

where L_j , ϵ_e , ϵ_p , ϵ_B are the luminosity of the jet $L_j = \eta \dot{M} c^2$, η is the fraction of accretion energy to the jet kinetic luminosity, the energy density of the electron, the energy density of the proton and the energy density of the magnetic field, respectively. We consider the energy flux is injected into the jet by the Blandford-Znajek process, and thus, the injected energy flux is proportional to the $\sin^2 \theta$. We consider the blob size at the base of the jet to be $R_{\text{blob}} \approx R_g$, and the length of the reconnection region in the vicinity of the BH is $r_{\text{rec}} \approx 2R_g$. Then, the angle of the blob to the reconnection region is estimated to be $\tan \theta = R_{\text{blob}}/r_{\text{rec}} \approx 0.5 \approx \theta$. We estimate the fraction to be $\eta = \int_{\pi/2-\theta}^{\pi/2} \sin^2 \theta d\theta / (\int_0^{\pi/2} \sin^2 \theta d\theta) \approx 0.58$. The magnetic energy density is written as $\epsilon_B = B^2/(8\pi) = 0.5(\epsilon_e + \epsilon_p)\tilde{\sigma}$, and thus, we estimate the magnetic field to be

$$B = \sqrt{\frac{L_j}{1 + 0.5\tilde{\sigma}}} \frac{4\pi\tilde{\sigma}}{\pi R_b^2 c}. \quad (2)$$

2.3 Particle Distribution

Because of the energy conservation, the number density of the particles at the base of the jet is estimated to be

$$n_e^0 \simeq \frac{L_j}{1 + 0.5\tilde{\sigma}} \frac{1}{\pi R_b^2 c} \frac{1}{m_e c^2}, \quad (3)$$

where the σ is the steady-state magnetization parameter estimated by the Eq.(20) of [5]. Next, we estimate the number density of particles at the dissipation region. We assume the charge neutrality, $\tilde{n}_e = \tilde{n}_p$. Since the proton mass is much higher than the electron mass, we consider the sum of the energy density of the electron and proton is written as $\epsilon_e + \epsilon_p \sim \tilde{n}_p m_p c^2$. We estimate the number density of the electron to be

$$\tilde{n}_e = \tilde{n}_p \simeq \frac{L_j}{1 + 0.5\tilde{\sigma}} \frac{1}{m_p c^2} \frac{1}{\pi R_b^2 c}. \quad (4)$$

In this study, we use the number density of electrons as $n_e = \max(n_e^0, \tilde{n}_e)$.

To obtain the energy distribution of nonthermal particles, we solve the steady-state transport equation:

$$-\frac{d}{d\gamma} \left(\frac{\gamma N_e(\gamma)}{t_{\text{cool}}} \right) = \dot{N}_{e,\text{inj}} - \frac{N_e(\gamma)}{t_{\text{esc}}}, \quad (5)$$

where $N_e(\gamma)$ is the differential number density of electrons, t_{cool} is the cooling time, and t_{esc} is the escape time of electrons from the blob. The analytic solution of this equation is given in Eq.(C.11) in the [9]. We consider the cooling process of the electron as synchrotron radiation and synchrotron self-Compton scattering, and thus, we calculate the cooling time as $t_{\text{cool}}^{-1} = t_{\text{syn}}^{-1} + t_{\text{IC}}^{-1}$. We calculate the t_{IC} given by subsection 2.6 of [10]. The escape time is estimated to be $t_{\text{esc}} = R_b/c$. In this study, the blob size is estimated to be $R_b = ct_v \delta_D \simeq 100R_g$, where t_v is the variability timescale

and δ_D is the Doppler factor. We use the variability timescale as the free parameter. For M87, the distance between the jet and the black hole is considered as $z \approx R^{3/2}$ from the observations of the jet ([11, 12]), and thus, we consider the distance $z \simeq 1000R_g$ for $R_b = 100R_g$. We estimate the Lorentz factor Γ of the jet at $z \simeq 1000R_g$ to be approximately $\Gamma\beta \simeq 0.8$ ([13]). The jet angle of the M87 is estimated as $\theta_j \approx 17$ deg by the observation of jet and counter jet proper motions ([14]), and thus, the Doppler factor is estimated to be $\delta_D \approx 1.9$.

The injection term of the transport equation is written as

$$\dot{N}_{e,\text{inj}} = \dot{N}_0 \begin{cases} \left(\frac{\gamma}{\gamma_{\min}}\right)^2 (\gamma < \gamma_{\min}) \\ \left(\frac{\gamma}{\gamma_{\min}}\right)^{-p} \exp\left(-\frac{\gamma}{\gamma_{\max}}\right) (\gamma > \gamma_{\min}) \end{cases}, \quad (6)$$

where the minimum and maximum Lorentz factors are assumed to be $\gamma_{\min} = (\delta B/B)^2 n_p m_p / (n_e m_e) \tilde{\sigma}$ and $\gamma_{\max} = \xi (\delta B/B)^2 \sigma$, respectively. The δB is the amplitude of the turbulent magnetic field, and the ξ represents the effect of the density reduction due to the expansion of the blob by the velocity dispersion of the blob. We calculate the normalization, \dot{N}_0 , as $\dot{N}_e = n_e \pi R_b^2 c = \int_1^\infty \dot{N}_{e,\text{inj}} d\gamma$. We calculate the luminosity of the electron as $L_e = \int_1^\infty \dot{N}_{e,\text{inj}} \gamma m_e c^2 d\gamma$, and we restrict it not to exceed the sum of the electron and proton luminosity $L_h = (\epsilon_e + \epsilon_p) \pi R_b^2 c = L_j / (1 + 0.5 \tilde{\sigma})$. We consider that the accelerated particles are power-law distribution at a certain σ , and the injection of these accelerated particles continues from σ to $\tilde{\sigma}$. Hence, we consider that the superposition of these particle distributions has the index p . In this study, we do not consider the radiation from protons since protons escape from the blob before they emit photons by synchrotron cooling.

3. Results

We apply the Jet-MAD model to the M87 and show the result in Figure 2. We tabulate the parameters and the physical quantities for M87 in Table 1. Figure 2 shows that the thermal synchrotron radiation from the MAD and the synchrotron radiation by the jet can explain the radio data. Synchrotron radiation from the jet can explain the optical to ultraviolet and soft X-ray data. Synchrotron radiation by nonthermal electrons and nonthermal protons from MAD can explain hard X-rays data and GeV gamma-ray data, respectively. Synchrotron radiation from the electron-positron pairs produced by the Bethe-Heitler process in the MAD can explain the TeV gamma-ray data. Synchrotron self-Compton in the jet does not work due to the high magnetic energy density.

Table 1: The list of the parameters and the physical quantities of the Jet-MAD model for M87.

Parameters of the Jet-MAD model								
\dot{m}	$M [M_\odot]$	r	s_{inj}	$\tilde{\sigma}$	p	ξ	$\delta B/B$	t_v
6×10^{-5}	6.3×10^9	10	1.4	0.01	2.18	10^3	0.33	2×10^6
Physical quantities								
σ	$B_{\text{jet}} [\text{G}]$	$n_e [1/\text{cm}^3]$	$L_j [\text{erg/s}]$	$L_e [\text{erg/s}]$	δ_D			
1.0×10^5	0.05	14.5	2.8×10^{43}	1.3×10^{41}	1.9			

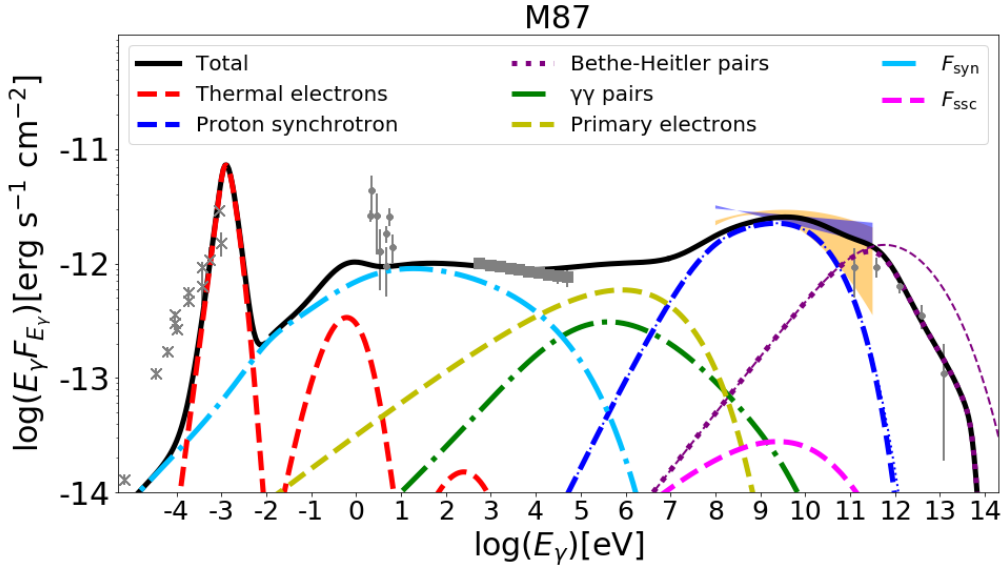


Figure 2: Photon spectrum fit to the M87. The thick and thin lines are the photon spectra after and before internal attenuation by the two-photon interaction, respectively. Gray points are the simultaneous observational data taken from [15]. Blue and orange shaded regions are power-law and log-parabola fitting spectrum taken from the Fermi-4FGL-DR3 catalog (https://fermi.gsfc.nasa.gov/ssc/data/access/lat/12yr_catalog/).

3.1 Different Acceleration mechanism

As mentioned above, the particle acceleration mechanism in the jet is still under debate. So far, we assume magnetic reconnection as the acceleration mechanism. We consider the two different acceleration mechanisms and apply them to M87.

3.1.1 Acceleration by the Alfvén wave dissipation

We consider the Alfvén waves to be generated by the accretion flows or by the wind and propagate along the magnetic field lines around the jet. The propagating Alfvén wave splits into a forward sound wave and a backward Alfvén wave due to the mode decay. The backward Alfvén wave and the forward Alfvén wave interact with each other and result in Alfvén turbulence inside the blob. We consider that the particles are accelerated by the dissipation of these Alfvén waves. For efficient mode decay, the amplitude of the magnetic field perturbation must be low for the highly magnetized plasma. Therefore, we assume $\delta B/B \simeq 0.01$, and thus, the maximum energy of the particle is much lower than that of the magnetic reconnection. We show the result in Fig.3 and find that the maximum energy is too low to explain the soft X-rays data due to the inefficient acceleration by the Alfvén wave dissipation.

3.1.2 Acceleration by the Magnetic reconnection

Recent particle-in-cell simulations show that the differential number density of particles has power-law tail beyond the maximum energy ([16]). We assume the index of the power-law tail as 2.5 or 3.0 and apply it to the M87. We show the results in Figure.4. This result shows that

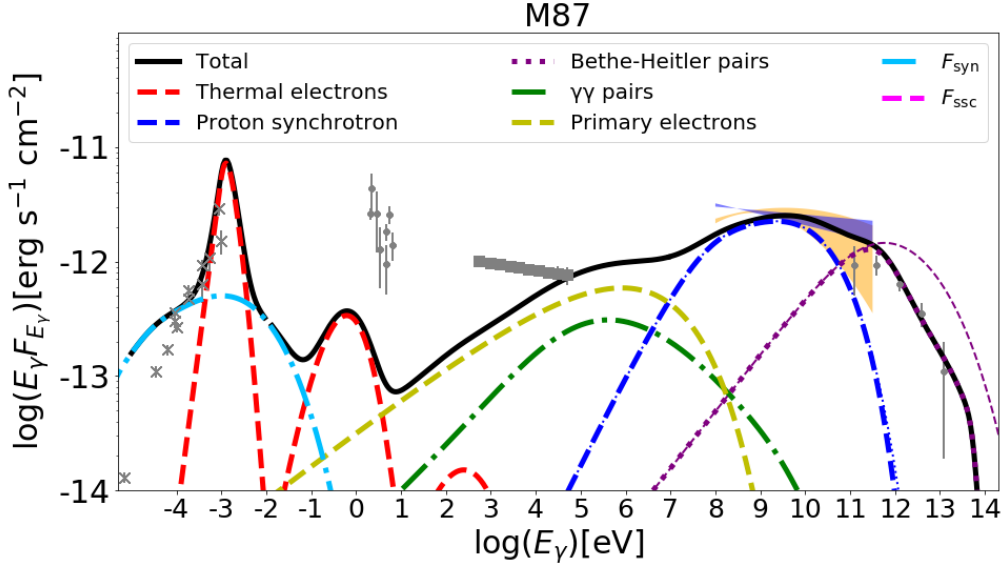


Figure 3: Same as Figure 2, but with the acceleration by the Alfvén wave dissipation.

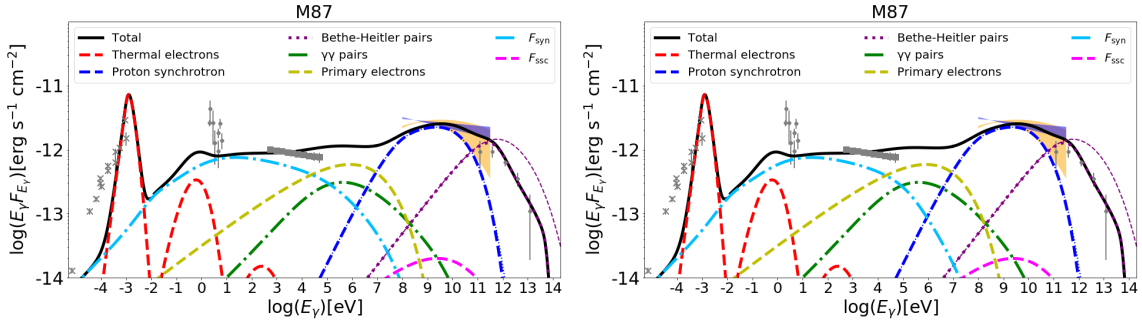


Figure 4: Same as Figure 2, but with the power-law tail beyond the maximum energy. The left and right panels are the photon spectra with the power-law tail index is 2.5 and 3.0, respectively.

the Jet-MAD model can explain the multi-wavelength observational data even if the differential number density has the power-law tail. We consider that magnetic reconnection is favored as the acceleration mechanism.

4. Summary and Discussion

We construct the two-zone Jet-MAD hybrid multi-wavelength emission model that takes into account the emission from the blob, which consists of electron-positron pairs produced by magnetic reconnection near the BH magnetosphere, and the emission from the MAD around the BH. We find that the Jet-MAD model can explain the simultaneous multi-wavelength observational data for M87.

This result suggests that the jet is composed of electron-positron pairs produced by magnetic reconnection in the vicinity of the BH magnetosphere and electron-protons injected from outside

the jet by the KHI. The maximum energy of protons γ_{\max} is about 10^7 , and the neutrino production by the photopion process ($p + \gamma \rightarrow p + \pi$) requires about 10eV photons. However, the number density of the 10eV photons is low, and thus, we consider the neutrino emission from the jet to be inefficient. Synchrotron radiation from jets can explain the optical, UV, and soft X-ray observational data. Synchrotron radiation by the nonthermal electrons and protons can explain the hard X-rays to gamma-ray observational data. We consider that the lower the energy of photons is, and farther the emission region is.

In addition, we consider the two different acceleration mechanisms and apply them to the M87. We find that the Alfvén wave dissipation acceleration scenario is disfavored because the Jet-MAD model cannot explain the observational data in this case. We consider the other acceleration mechanism as magnetic reconnection. In this case, the Jet-MAD model can explain the observational data for both the exponential cut-off and the power-law tail. This result suggests that magnetic reconnection scenario is favored as the acceleration mechanism inside the blob. The soft power-law index is required to explain the observational data, and thus, we consider that more energy is released to the particles for the lower magnetization parameter.

References

- [1] MAGIC Collaboration, Acciari, V. A., Ansoldi, S., et al. 2020, MNRAS, 492, 5354
- [2] Kimura, S. S., & Toma, K. 2020, ApJ, 905, 178
- [3] Kuze, R., Kimura, S. S., & Toma, K. 2022, ApJ, 935, 159
- [4] Kimura, S. S., Toma, K., Noda, H., & Hada, K. 2022, ApJL, 937, L34
- [5] Chen A. Y. , Uzdensky D., Dexter J., 2023, ApJ , 944, 173
- [6] Ripperda, B., Liska, M., Chatterjee, K., et al. 2022, ApJL, 924, L32
- [7] Blandford, R., Meier, D., & Readhead, A. 2019, ARA&A, 57, 467
- [8] Kazuhiro Hada. Relativistic Jets from AGN Viewed at Highest Angular Resolution. Galaxies, 8(1):1, December 2019.
- [9] Dermer, C. D., & Menon, G. 2009, High Energy Radiation from Black Holes: Gamma Rays, Cosmic Rays, and Neutrinos (Princeton, NJ: Princeton Univ. Press)
- [10] Blumenthal, G. R., & Gould, R. J. 1970, Rev. Mod. Phys., 42, 237
- [11] Hada, K., Kino, M., Doi, A., et al. 2013, ApJ, 775, 70
- [12] Nakamura, M., Asada, K., Hada, K., et al. 2018, ApJ, 868, 146
- [13] Park, J., Hada, K., Kino, M., et al. 2019, ApJ, 887, 147
- [14] Walker, R. C., Hardee, P. E., Davies, F. B., Ly, C.,& Junor, W. 2018, ApJ, 855, 128
- [15] EHT MWL Science Working Group, Algaba, J. C., Añczarski, J., et al. 2021, ApJL, 911, L11
- [16] Hakobyan, H., Petropoulou, M., Spitkovsky, A., & Sironi, L. 2021, ApJ, 912, 48,